See related commentary on pg 2357

Inactivation of the Vitamin D Receptor Enhances Susceptibility of Murine Skin to UV-Induced Tumorigenesis

Tara I. Ellison[1], Molly K. Smith[2], Anita C. Gilliam[2] and Paul N. MacDonald[1]

1,25-Dihydroxyvitamin D_3 ($1,25(OH)_2D_3$) is the biologically active ligand for the vitamin D receptor (VDR). $VDR^{-/-}$ mice have a hair follicle-cycling defect resulting in alopecia. However, mice lacking 25-hydroxyvitamin D_3 1α-hydroxylase ($CYP27B1^{-/-}$), and having no circulating $1,25(OH)_2D_3$, have normal follicular function. These mouse models indicate that VDR functions independently of $1,25(OH)_2D_3$ in regulating hair-follicle cycling. Here, we show that $VDR^{-/-}$ mice rapidly develop chemically induced skin tumors, whereas $CYP27B1^{-/-}$ and wild-type mice do not, indicating that VDR, and not the $1,25(OH)_2D_3$ ligand, is essential for protection against skin tumorigenesis. Because the majority of human skin cancer results from exposure to UV, the susceptibility of $VDR^{-/-}$ mice to this carcinogen was also evaluated. $VDR^{-/-}$ mice developed UV-induced tumors more rapidly and with greater penetrance than did $VDR^{+/+}$ mice. p53 protein levels were upregulated at similar rates in UV-treated keratinocytes of $VDR^{-/-}$ and $VDR^{+/+}$ mice. However, rates of thymine-dimer repair and UV-induced apoptosis were significantly lower in $VDR^{-/-}$ epidermis compared with the wild type epidermis. UV-induced epidermal thickening was also attenuated in $VDR^{-/-}$ skin, indicating that VDR plays a critical role in the repair and removal of severely damaged keratinocytes and adaptation of the skin to chronic UV exposure.

Journal of Investigative Dermatology (2008) **128,** 2508–2517; doi:10.1038/jid.2008.131; published online 29 May 2008

INTRODUCTION

Approximately one million people are diagnosed with non-melanoma skin cancer each year, which accounts for half of all diagnosed tumors. The incidence of non-melanoma skin cancer is increasing and, while rarely fatal, poses significant health care challenges (Albert and Weinstock, 2003). The vitamin D endocrine system protects against multiple forms of carcinogenesis, but its significance in skin tumorigenesis is only beginning to be appreciated (Zinser *et al.*, 2002; Bikle, 2004). In addition, the molecular mechanisms that govern the activity of the vitamin D endocrine system in the skin remain unclear.

The biologically active form of vitamin D is 1,25-dihydroxyvitamin D_3 ($1,25(OH)_2D_3$). This hormone binds the vitamin D receptor (VDR) and promotes association with its heterodimeric partner, the retinoid X receptor (Kliewer *et al.*, 1992; Cheskis and Freedman, 1994). The VDR–retinoid X receptor heterodimer regulates transcription by binding to specific response elements in the promoter regions of target genes (Kerner *et al.*, 1989). Synthesis of $1,25(OH)_2D_3$ is highly regulated and involves several tissues. Vitamin D prohormone is produced primarily in the skin, where 7-dehydrocholesterol is converted to vitamin D by UV light. Bioactivation of vitamin D occurs through sequential hydroxylation at C-25 in the liver and at C-1 in the kidney (Holick, 2007). The renal 25-hydroxyvitamin D 1α-hydroxylase (1αOHase) enzyme is required to generate circulating levels of $1,25(OH)_2D_3$ in humans and other mammals (Gray *et al.*, 1972; St-Arnaud *et al.*, 1997; Dardenne *et al.*, 2001; Panda *et al.*, 2001).

Knockout mouse models have provided important physiological insights into the vitamin D endocrine system. Four independent strains of mice have been generated in which the VDR has been inactivated (that is, receptor-knockout mice) (Li *et al.*, 1997; Yoshizawa *et al.*, 1997; Van Cromphaut *et al.*, 2001; Erben *et al.*, 2002). Two additional strains of mice were engineered to target the *CYP27B1* gene, which encodes the renal 1αOHase enzyme (that is, ligand-knockout mice) (Dardenne *et al.*, 2001; Panda *et al.*, 2001). $CYP27B1^{-/-}$ mice are devoid of circulating $1,25(OH)_2D_3$. As expected, receptor- and ligand-knockout mice have similar phenotypes relating to mineral homeostasis, manifesting as hypocalcemia, hyperparathyroidism, and skeletal defects such as rickets. Interestingly, this phenotype is corrected by feeding the mice a diet high in calcium, phosphorus, and lactose, suggesting that the significance of the vitamin D endocrine system in the

[1]*Department of Pharmacology, Case Western Reserve University, Cleveland, Ohio, USA and* [2]*Department of Dermatology, Case Western Reserve University, Cleveland, Ohio, USA*

Correspondence: Dr Paul N. MacDonald, Department of Pharmacology, Case Western Reserve University, 10900 Euclid Avenue, Cleveland, Ohio 44116, USA. E-mail: pnm2@case.edu

Abbreviations: $1,25(OH)_2D_3$, 1,25-dihydroxyvitamin D_3; AFX, atypical fibroxanthoma; DMBA, dimethylbenzanthracene; PBS, phosphate-buffered saline; SCC, squamous cell carcinoma; VDR, vitamin D receptor; 1αOhase, 25-hydroxyvitamin D_3-1α-hydroxylase

Received 15 October 2007; revised 24 March 2008; accepted 27 March 2008; published online 29 May 2008

skeletal system is secondary to its role in maintaining adequate absorption of dietary calcium by the intestine (Li *et al.*, 1998; Dardenne *et al.*, 2003).

Importantly, the VDR- and ligand-knockout mice ($VDR^{-/-}$ and $CYP27B1^{-/-}$, respectively) differ greatly in their skin phenotypes. $VDR^{-/-}$ mice develop an initial postnatal coat of hair, but subsequent hair-follicle cycling fails leading to alopecia (Li *et al.*, 1998). Hair follicles degenerate to form dermal cysts and utriculi (Li *et al.*, 1998), and epidermal keratinocytes proliferate at approximately twice the normal rate (Zinser *et al.*, 2002). This phenotype is not corrected by a high-calcium diet, indicating that it is a direct consequence of VDR inactivation (Li *et al.*, 1998). In contrast, $CYP27B1^{-/-}$ mice have normal hair-follicle cycling, a normal keratinocyte proliferative index, and display only minor differences in the expression of skin differentiation marker proteins (Bikle *et al.*, 2004). The lack of phenotype in $CYP27B1^{-/-}$ skin, as compared with the $VDR^{-/-}$ skin, strongly suggests that VDR regulates transcription in keratinocytes independently of its $1,25(OH)_2D_3$ ligand. Indeed, recent data demonstrating a $1,25(OH)_2D_3$-independent transcriptional activity of the VDR selectively in human and mouse keratinocytes provide key support for this concept (Ellison *et al.*, 2007).

Genetic inactivation of VDR also increases susceptibility of mice to chemically induced skin tumorigenesis. $VDR^{-/-}$ mice rapidly develop skin tumors following oral administration of dimethylbenzathracene (DMBA), whereas wild-type mice are resistant to tumor development (Zinser *et al.*, 2002). Pharmacological doses of $1,25(OH)_2D_3$ have been shown to increase latency and reduce multiplicity of chemically induced skin tumor formation in mice (Chida *et al.*, 1985). However, it is presently unknown whether $CYP27B1^{-/-}$ mice show altered susceptibility to DMBA-induced skin carcinogenesis. Although chemical carcinogenesis protocols provide a convenient way to study tumorigenesis in rodents over a relatively short time period, the major environmental risk factor in human skin carcinogenesis is exposure to UV light (Albert and Weinstock, 2003). UV light, particularly UVB with wavelengths between 290 and 320 nm, causes DNA damage, including formation of cyclobutane pyrimidine dimers (Setlow and Setlow, 1962) and (6–4) photoproducts (Johns *et al.*, 1964). Failure to adequately repair or remove a damaged cell may yield a mutated cell with the potential ability to clonally expand and become tumorigenic. Therefore, it is critical to evaluate whether VDR also plays a protective role against UV-induced tumorigenesis, and if so, to evaluate the mechanisms underlying this protective activity of VDR.

In this report, we provide evidence that VDR, but not its $1,25(OH)_2D_3$ ligand, is required for *in vivo* resistance to chemically induced skin tumorigenesis in mice. Furthermore, we show that VDR is essential for protection against UV-induced skin carcinogenesis. This striking difference in UV-induced tumor susceptibility may be due, in part, to a significant reduction in thymine-dimer repair and keratinocyte apoptosis in $VDR^{-/-}$ skin following acute exposure to UV light. In addition, $VDR^{-/-}$ skin shows reduced epidermal thickening in response to repeated UV exposure, indicating that $VDR^{-/-}$ skin does not mount an appropriate protective response to UV, leaving basal keratinocytes more exposed to penetrating UV rays.

RESULTS

Protection against chemically induced skin tumorigenesis is VDR-dependent and 1αOHase-independent in mice

$VDR^{-/-}$ mice are more susceptible to chemically induced skin carcinogenesis compared with wild-type mice (Zinser *et al.*, 2002), suggesting a genoprotective role for VDR in the skin. However, the significance of the 1αOHase enzyme, and thus the $1,25(OH)_2D_3$ ligand, in preventing skin tumor development is not known. Therefore, we compared skin tumor development in wild-type, $VDR^{+/-}$, $VDR^{-/-}$, $CYP27B1^{+/-}$, and $CYP27B1^{-/-}$ mice receiving two oral doses of the chemical carcinogen DMBA using a dosing regimen described previously for $VDR^{-/-}$ mice (Zinser *et al.*, 2002). Mice were monitored for skin tumor development on a weekly basis. All $VDR^{-/-}$ mice developed skin tumors within 10–12 weeks after receiving DMBA (Figure 1a). A representative $VDR^{-/-}$ mouse bearing multiple tumors is

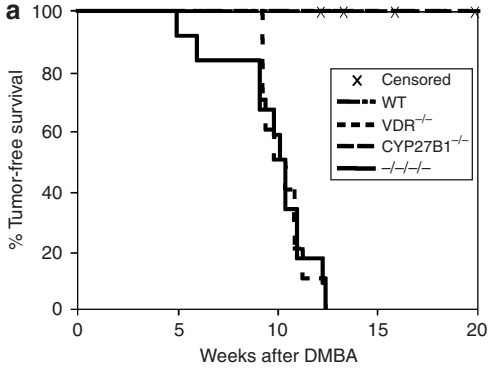

Figure 1. Protection against chemically induced skin tumorigenesis is VDR-dependent and 1αOHase-independent in mice. $VDR^{+/+}$ ($n=11$), $VDR^{+/-}$ ($n=6$), and $VDR^{-/-}$ mice ($n=10$); $CYP27B1^{+/+}$ ($n=10$), $CYP27B1^{+/-}$ ($n=11$), and $CYP27B1^{-/-}$ mice ($n=10$); and $VDR^{-/-}$ $CYP27B1^{-/-}$ mice ($n=13$) were given two doses of DMBA by oral gavage at 5 and 6 weeks of age. Mice were monitored weekly by palpation and visual inspection for tumor development. (**a**) Probability of tumor development was analyzed according to the method of Kaplan–Meier. $VDR^{+/+}$ and $CYP27B1^{+/+}$ mice were grouped for statistical analysis. Mice were censored if they died or if they required euthanasia due to extreme sickness before developing a skin tumor. (**b**) A representative image of a $VDR^{-/-}$ mouse bearing several DMBA-induced skin tumors.

shown in Figure 1b. Skin tumors were classified as sebaceous hyperplasias (15%), adenomas (70%), or carcinomas (5%) depending on the ratio of well-differentiated sebocytes to epithelial keratinocytes. These tumors, like many of the tumors previously reported in $VDR^{-/-}$ skin (Zinser *et al.*, 2002), likely originated from the folliculosebaceous unit. In addition, 10% of tumors were classified as warts due to signs of viral change, such as koilocytic change, church-spire parakeratin, and dilated blood vessels in the stroma. In striking contrast to $VDR^{-/-}$ mice, no skin tumors were observed in wild type or $CYP27B1^{-/-}$ mice during the 8 months of the study. In addition, no tumors were observed in mice heterozygous for the *VDR* or *CYP27B1* genes. Since $CYP27B1^{-/-}$ mice lack detectable levels of circulating $1,25(OH)_2D_3$ (Dardenne *et al.*, 2001; Panda *et al.*, 2001), these data indicate that VDR, but not its $1,25(OH)_2D_3$ ligand, is required for protection from DMBA-induced tumorigenesis. To test whether loss of $1,25(OH)_2D_3$ can further sensitize $VDR^{-/-}$ mice to tumorigenesis, we generated mice deficient in both *VDR* and *CYP27B1* (double knockout mice) and administered DMBA as described above. Average time to tumor development was virtually identical in $VDR^{-/-}$ and $VDR^{-/-}$ $CYP27B1^{-/-}$ mice (10.6 ($\pm$1.1) and 10.7 ($\pm$1.2) weeks after DMBA exposure, respectively). These data indicate that loss of $1,25(OH)_2D_3$ through genetic deletion of the 1αOHase enzyme does not increase susceptibility of mice to tumorigenesis whether or not they express the VDR.

VDR protects mice from UV-induced skin tumorigenesis

UV light causes the majority of human skin cancers, and as it both initiates and promotes tumorigenesis, is considered to be a complete carcinogen. To determine whether VDR protects the skin against UV-induced skin cancer, $VDR^{-/-}$ and wild-type mice were chronically exposed to UVB three times per week for 33 weeks, and monitored weekly for tumor development for 45 weeks. $CYP27B1^{-/-}$ mice were not included in this study as they lack an overt skin or hair phenotype, and as they are completely resistant to the aggressive, rapid-onset, chemically induced carcinogenesis paradigm.

$VDR^{+/+}$ and $VDR^{-/-}$ mice were shaved and depilated as needed to maintain bare skin during the course of thrice-weekly UV treatments. $VDR^{-/-}$ mice began to develop tumors after approximately 18 weeks of UV exposure, and half of the $VDR^{-/-}$ mice had developed at least one tumor by 30 weeks into the study (Figure 2a). All of the $VDR^{-/-}$ mice that completed the 45-week study developed at least one tumor. In contrast, only three wild-type mice developed tumors by this time, and these tumors appeared much later than those in the $VDR^{-/-}$ mice (36–44 weeks after the start of UV). All but one of the $VDR^{-/-}$ tumors were classified as squamous in origin (Table 1). Sixty percent of $VDR^{-/-}$ tumors were squamous papillomas, with various degrees of atypia and dysplasia. Benign papillomas (Figure 2d) typically had a larger amount of keratinized material than more atypical papillomas, indicating a greater degree of cellular differentiation. The moderate papillomas contained parakeratin, indicative of a defect in the differentiation process (Figure 2f). Moderate papillomas also contained more proliferating-cell nuclear antigen (PCNA)-positive cells than benign papillomas (Figure 2g and e, respectively), indicating a higher proliferative index. Nearly 20% of $VDR^{-/-}$ tumors were malignant squamous cell carcinomas (SCCs) *in situ*, showing high degree of atypia, many mitotic figures, and disordered skin structure. An additional 20% of $VDR^{-/-}$ tumors were invasive SCCs containing a large percentage of proliferating cells (Figure 2i), significant atypia and disordered structure, and invasion of the surrounding tissue (Figure 2h). One invasive SCC was observed in a wild-type mouse, but the remaining $VDR^{+/+}$ tumors were a dermal hyperproliferation, with characteristics consistent with atypical fibroxanthoma (AFX). These tumors had a high proliferative index, as shown by the large number of PCNA-expressing cells (Figure 2k), a disordered growth pattern, and in some cases contained black pigmentation (Figure 2j). One $VDR^{-/-}$ mouse developed this type of tumor, suggesting that AFX is not unique to the wild-type mice.

UV induces p53 protein levels equally in wild-type and $VDR^{-/-}$ keratinocytes

Tumorigenesis occurs after normal cells have sustained multiple insults and have been subject to growth promotion (Matsumura and Ananthaswamy, 2002). Therefore, long-term susceptibility to tumorigenesis may be determined by the ability of the skin to deal with acute UV-induced damage. DNA damage causes stabilization and upregulation of the p53 tumor-suppressor protein (Maltzman and Czyzyk, 1984). Phosphorylation increases p53 protein stability and transcriptional activity (Siliciano *et al.*, 1997). Active p53 either halts the cell cycle so that cellular damage can be repaired, or initiates apoptosis. To determine whether $VDR^{-/-}$ mice have a defect in the p53 response, primary mouse keratinocytes were isolated from wild-type and $VDR^{-/-}$ mice. Cells were exposed to UVB and protein was harvested at various time points. Western blot analysis indicated that p53 was upregulated as early as 4 hours after UV exposure, protein levels peaked at 8 hours, and subsequently declined at 24 and 48 hours (Figure 3). Notably, p53 levels were similar in $VDR^{+/+}$ and $VDR^{-/-}$ keratinocytes. We also observed UV-induced increases in the levels of phosphorylated serine 15 p53 that were comparable in wild-type and $VDR^{-/-}$ keratinocytes at each time point after UV exposure (Figure 3), suggesting that this important, early response to UV in keratinocytes is not dramatically altered in $VDR^{-/-}$ keratinocytes.

Incomplete repair of thymine dimers in $VDR^{-/-}$ epidermis as compared with wild type

p53 upregulation institutes cell-cycle arrest, which allows time for DNA repair. If UV-induced thymine dimers are not repaired before a cell replicates, this damage transforms into permanent mutations in the genetic code. To address an *in vivo* role of VDR in thymine-dimer repair, wild-type and $VDR^{-/-}$ newborn mice were irradiated with UV and skin was harvested at the indicated time points. Genomic DNA was isolated from the epidermis and thymine dimers were

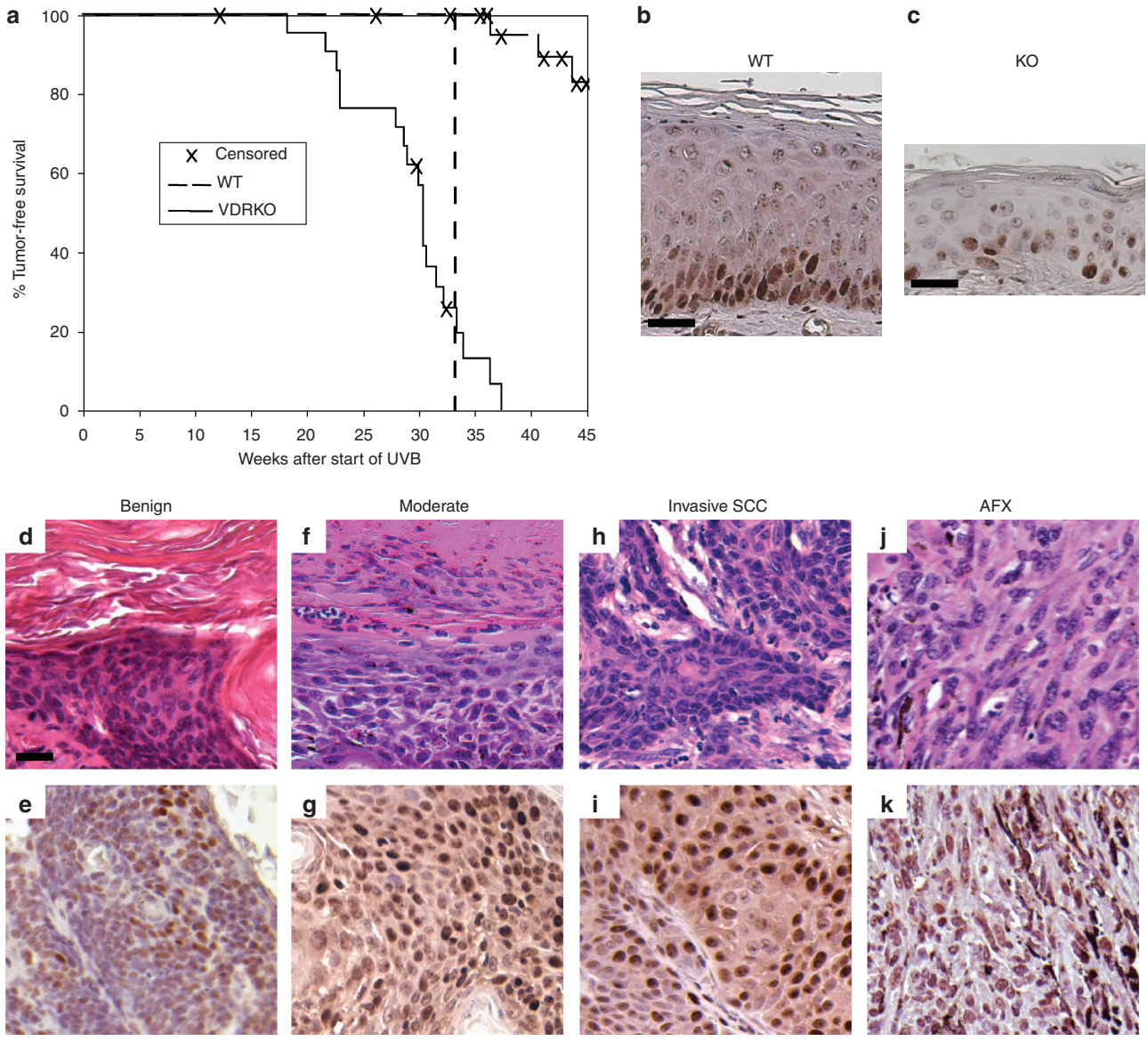

Figure 2. VDR protects mice from UV-induced skin tumorigenesis. (**a**) $VDR^{+/+}$ ($n = 23$) and $VDR^{-/-}$ ($n = 22$) mice were shaved and treated with a depilatory lotion, and then exposed to UV thrice weekly for 33 weeks as described under Materials and Methods. Mice were monitored weekly by palpation and visual inspection for tumor development. Probability of tumor development was analyzed according to the method of Kaplan–Meier. Mice were censored if they died or if they required euthanasia due to extreme sickness before developing a skin tumor. (**b**) Representative image of thickened but non-tumor-bearing skin from a wild-type mouse after 26 weeks of regular UV exposure. Bar = 20 μm. (**c**) Representative image of thickened but non-tumor-bearing skin from a $VDR^{-/-}$ mouse after 29 weeks of regular UV exposure. Bar = 20 μm. Histological appearance of a representative benign papilloma (**d**, **e**), moderate papilloma (**f**, **g**), an invasive SCC (**h**, **i**), and an AFX (**j**, **k**). Images were taken of hematoxylin and eosin-stained paraffin-embedded sections (**d**, **f**, **h**, **j**), and of sections immunohistochemically stained with an antibody against PCNA to indicate proliferation (**e**, **g**, **i**, **k**). PCNA-positive cells appear brown. Bar (**d**–**k**) = 20 μm.

Table 1. Histological classification of tumors induced by UV irradiation in wild-type and $VDR^{-/-}$ mice

	Papilloma							
	Benign	Mild	Moderate	Severe	SCC *in situ*	Inv SCC	AFX	Total
WT	0	0	0	0	0	1	3	4
KO	4	5	6	1	5	5	1	27

AFX, atypical fibroxanthoma; KO, knockout; SCC, squamous cell carcinoma; VDR, vitamin D receptor; WT, wild type.

quantified by southwestern slot blotting using an antibody recognizing this form of DNA damage. As expected, untreated epidermis lacked detectable thymine dimers (Figure 4). In wild-type epidermal samples, the levels of thymine dimer were highest immediately following irradiation, and gradually decreased over time, nearly returning to baseline levels at 24 hours after irradiation. In contrast, levels of thymine dimers were higher in $VDR^{-/-}$ epidermis as compared with the wild type at each time point, and the amount of thymine dimers remained significantly higher in

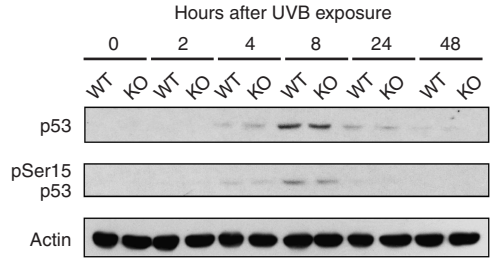

Figure 3. UV induces p53 protein levels and p53 phosphorylation equally in wild-type and VDR$^{-/-}$ keratinocytes. Keratinocytes were isolated from newborn wild-type and VDR$^{-/-}$ mice, allowed to grow for 24 hours, and irradiated with 50 mJ cm^{-2} of UVB through a thin film of PBS. Media were replaced and protein was harvested at the indicated time points. Protein expression was analyzed by western blotting.

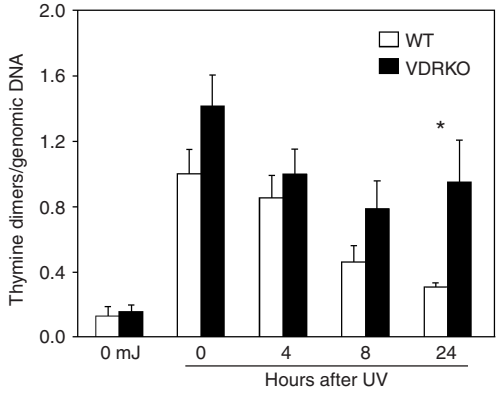

Figure 4. Incomplete repair of thymine dimers in VDR$^{-/-}$ epidermis compared with wild type. Newborn mice were exposed to 120 mJ cm^{-2} of UV and skin was collected at the indicated time points. Epidermal genomic DNA was isolated and thymine dimers were measured by southwestern slot blot. Thymine dimers were normalized to total genomic DNA with a radiolabeled mouse genomic DNA probe. Thymine dimers were measured in the epidermis of 2–3 individual mice for each time point, except for the unirradiated control. The data shown represent the mean from three independent measurements of thymine dimers relative to total genomic DNA from the epidermal samples. Error bars represent SEM; *$P<0.04$.

VDR$^{-/-}$ epidermis than in the wild type at 24 hours after UV exposure (Figure 4), indicating that keratinocyte DNA-repair pathways are compromised by VDR ablation.

UVB-induced growth arrest is compromised in VDR$^{-/-}$ keratinocytes *in vitro*

Growth arrest is a critical, immediate response of keratinocytes to UV exposure so that effective repair of the damage may occur prior to DNA replication (Petrocelli *et al.*, 1996). Failure to provide this important window for repair leads to propagation of the damage and cancer. Therefore, we tested whether VDR$^{-/-}$ keratinocytes displayed altered proliferative responses to UV exposure *in vitro*. Wild-type and VDR$^{-/-}$ keratinocytes were irradiated once with various doses of UVB and proliferation was monitored for 3 days using the MTT assay. Confirming previous reports (Sakai and Demay, 2000), non-irradiated wild-type and VDR$^{-/-}$ keratinocytes grew at similar rates *in vitro* (Figure 5a and b). Exposure of VDR$^{+/+}$

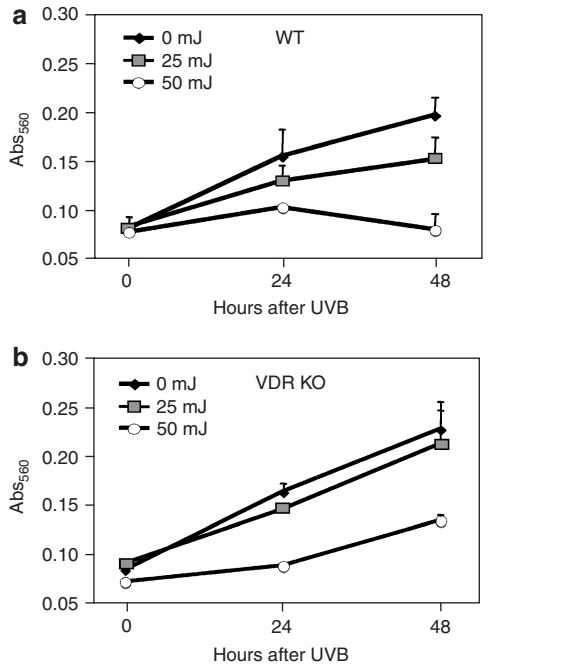

Figure 5. UVB-induced growth arrest is compromised in VDR$^{-/-}$ keratinocytes *in vitro*. Primary keratinocytes were isolated from newborn wild-type and VDR$^{-/-}$ mice, allowed to grow for 24 hours, and irradiated with the indicated amount of UVB through a thin film of PBS. Media were replaced and cell proliferation was measured at the indicated time points using the MTT assay as described under Materials and Methods. Cell growth of (**a**) wild-type and (**b**) VDR$^{-/-}$ keratinocytes is plotted over time. Error bars represent SD.

keratinocytes to a 25-mJ cm^{-2} dose of UVB attenuated their growth rate at 24 and 48 hours following a single UV exposure. In contrast, VDR$^{-/-}$ keratinocytes were virtually unaffected by this dose of UVB. A higher level of UVB exposure (50 mJ cm^{-2}) effectively blocked the growth of wild-type keratinocyte at 24 and 48 hours (Figure 5a). The VDR$^{-/-}$ keratinocytes continued to grow at this higher UV dose, albeit more slowly (Figure 5b). These data indicate that VDR$^{-/-}$ keratinocytes are defective in UV-induced growth arrest as compared with their wild-type counterparts.

In vivo apoptotic defects in VDR$^{-/-}$ keratinocytes following a single dose of UV

In addition to growth arrest and repair, keratinocytes undergo apoptosis if cellular damage is too severe to be repaired. Figure 6 illustrates proliferative and apoptotic responses of keratinocytes *in vivo* following exposure of VDR$^{+/+}$ and VDR$^{-/-}$ mice to a single dose of UVB. Shaved and depilated dorsal skin of wild-type and VDR$^{-/-}$ mice were exposed to a 120-mJ cm^{-2} dose of UV and skin was harvested 24 hours later. Proliferative keratinocytes were visualized by PCNA staining. Apoptotic cells were fluorescently labeled by the TUNEL method and nuclei were counterstained with 4, 6-diamino-2-phenylindole. Differences in proliferation were not apparent *in vivo*, perhaps due to the nature of this single, high dose of UVB (Figure 6a). However, VDR$^{-/-}$ skin contained less than half the number of apoptotic

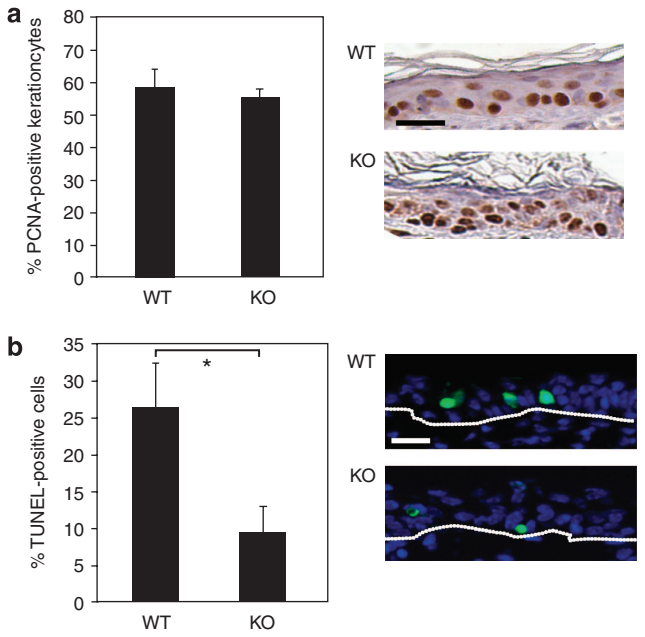

Figure 6. *In vivo* apoptotic defects in VDR$^{-/-}$ keratinocytes following a single dose of UV. Wild-type (WT, $n=4$) and VDR$^{-/-}$ (KO, $n=4$) mice were exposed to 120 mJ cm^{-2} of UV and a biopsy was collected 24 hours later. (**a**) Skin samples were stained for PCNA expression and counterstained with hematoxylin (positive cells are brown). PCNA-positive keratinocytes in WT and KO skin were counted as a percentage of total number of keratinocytes. Error bars represent SEM. Representative sections are shown on the right. Bar = 20 μm. (**b**) Apoptotic cells were labeled by the TUNEL method and nuclei were counterstained with 4,6-diamino-2-phenylindole. Apoptosis rates were calculated as the number of TUNEL-positive cells as a percentage of total epidermal keratinocytes from multiple fields of TUNEL-labeled, paraffin-embedded skin sections, viewed at an original magnification of ×100. Error bars represent SD. Differences were analyzed by the two-tailed Student's *t*-test; *$P=0.005$. Representative fields of TUNEL-labeled sections are on the right, showing TUNEL-positive cells in green and nuclei in blue. Bar = 20 μm. Dotted lines indicate the epidermal–dermal junction.

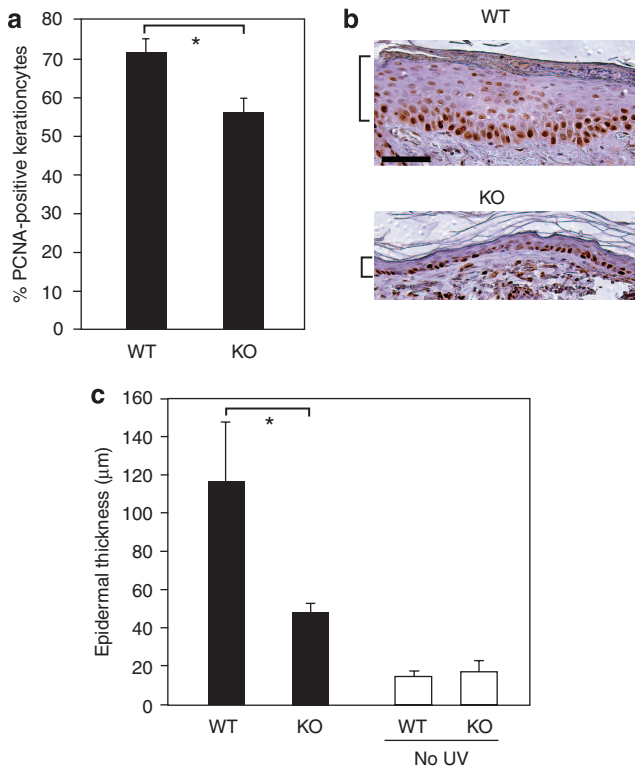

Figure 7. Defective epidermal thickening of VDR$^{-/-}$ skin in response to chronic UV exposure. Wild-type (WT, $n=4$) and VDR$^{-/-}$ (KO, $n=4$) mice were exposed to six doses of UV (120 mJ cm^{-2}) during a 2-week period. Skin samples were collected and fixed 24 hours after the final dose. (**a**) Skin samples were stained for PCNA expression and counterstained with hematoxylin. PCNA-positive keratinocytes in WT and KO skin were counted as a percentage of total number of keratinocytes. Wild-type epidermis was significantly more proliferative than VDR$^{-/-}$ epidermis following six exposures of UV; *$P<0.025$. Error bars represent SEM. Differences were analyzed by two-tailed Student's *t*-test. (**b**) Representative sections of wild-type and VDR$^{-/-}$ skin, stained for PCNA expression. Brackets indicate epidermal thickness. Bar = 40 μm. (**c**) Epidermal thickness was calculated from 20–25 measurements from multiple fields of paraffin-embedded skin sections, viewed at an original magnification of ×100. Error bars represent SD. Differences in thickness were analyzed by two-tailed Student's *t*-test. Wild-type epidermis was significantly thicker than VDR$^{-/-}$ epidermis following six exposures of UV, *$P<0.015$.

keratinocytes as compared with wild-type skin (Figure 6b). This finding suggests that tumor susceptibility in VDR$^{-/-}$ mice may also derive from a decreased ability to eliminate damaged cells from the skin due to defective keratinocyte apoptosis.

Defective epidermal thickening of VDR$^{-/-}$ skin in response to chronic UV exposure

Following UV-induced cell-cycle arrest and repair, keratinocytes enter a hyperproliferative stage in order to replace cell loss due to apoptosis (that is, sunburn cells) and to increase the number of epidermal cell layers to protect basal cells against additional UV exposure (de Winter *et al.*, 2001). Differences in the ability to adapt to chronic UVB exposure may explain the variation in long-term susceptibility to UV-induced tumorigenesis. Wild-type and VDR$^{-/-}$ mice (5–7 weeks old) were exposed to UVB six times over a period of 2 weeks. Skin samples were obtained 24 hours after the final dose, stained for PCNA expression to indicate proliferating cells, and epidermal thickness was measured. Representative sections of VDR$^{+/+}$ and VDR$^{-/-}$ skin after the final dose of UV are shown in Figure 7b. Virtually all keratinocytes in the basal layer were proliferating in both the VDR$^{+/+}$ and VDR$^{-/-}$ skin, but the wild-type epidermis contained an abundance of keratinocytes proliferating above the basal layer. This effect required repeated doses, since, as previously shown, PCNA-positive keratinocytes in the epidermal layers were similar in wild-type and VDR$^{-/-}$ epidermis following a single, acute, exposure to UVB (Figure 6a). Following more chronic exposure to six doses of UV, the PCNA-positive VDR$^{+/+}$ keratinocytes were at a level of 72%, whereas PCNA-positive VDR$^{-/-}$ keratinocytes were at a significantly lower level of 56% ($P< 0.025$; Figure 7a). These differences in the proliferative index correlated to differences in epidermal thickness between wild-type and VDR$^{-/-}$ skin. Average epidermal thickness was

similar in wild-type and $VDR^{-/-}$ mice that were not exposed to UV (14.7 ± 3.6 and 17.4 ± 5.4 μm, respectively) (Figure 7c). Differences in epidermal thickness of 24-hour $VDR^{+/+}$ and $VDR^{-/-}$ skin were not apparent following a single, acute, exposure 24 hours post UV treatment. However, following six doses of UV the average epidermal thickness of wild-type mice increased eightfold compared with that in unexposed mice, whereas average thickness in $VDR^{-/-}$ mice increased less than threefold. This indicates a significant difference in UV-induced epidermal thickening in wild-type mice as compared with $VDR^{-/-}$ mice. The reduced levels of keratinocyte proliferation and apoptosis in $VDR^{-/-}$ skin in response to UV exposure suggest that these mice do not mount a sufficient defense against the damage caused by UV radiation, which compounded over a chronic series of UV exposures leaves them more susceptible to UV-induced skin tumorigenesis.

DISCUSSION

Arguably, one of the most remarkable observations derived from the vitamin D endocrine system-knockout mouse models centers on the lack of a profound skin and hair phenotype in the $CYP27B1^{-/-}$ mice as compared with the defects observed in $VDR^{-/-}$ skin. These mouse models are consistent with rare genetic diseases resulting from inactivation of *VDR* and *CYP27B1* in humans. That is, many patients with hereditary vitamin D-resistant rickets (resulting from inactivating mutations of VDR) present with alopecia, whereas those with pseudo-vitamin D deficiency rickets (resulting from inactivation of the 1αOHase enzyme) do not (Hughes *et al.*, 1988; St-Arnaud *et al.*, 1997). Indeed, classic dietary deficiency studies over the past century support these more modern genetic approaches, in that vitamin D deficiency does not significantly impact skin or hair. These and other observations led to the hypothesis that VDR may act independently of $1,25(OH)_2D_3$ in keratinocytes. One of the most significant aspects of this study is that the ligand-independent nature of VDR function in the skin can now be extended to a second global process, namely, protection against chemically induced skin tumorigenesis. The $CYP27B1^{-/-}$ mice are remarkably resistant to chemically induced skin tumor development using a paradigm in which all of the $VDR^{-/-}$ mice developed multiple tumors per animal. Clearly, lack of systemic $1,25(OH)_2D_3$ has no impact on the sensitivity of mouse skin to chemically induced tumorigenesis, whereas lack of VDR does. Mechanisms involved in this difference in cancer susceptibility remain to be defined.

Several possibilities exist that explain the apparent uncoupling of VDR and $1,25(OH)_2D_3$ in both hair follicle cycling and in protection against DMBA-induced skin tumorigenesis. Whereas systemic $1,25(OH)_2D_3$ is undetectable in $CYP27B1^{-/-}$ mice (Dardenne *et al.*, 2001; Panda *et al.*, 2001), it is possible that local production of $1,25(OH)_2D_3$ occurs in the $CYP27B1^{-/-}$ keratinocytes. Keratinocytes synthesize $1,25(OH)_2D_3$ (Bikle *et al.*, 1986) where it may act in an autocrine/paracrine manner to control keratinocyte differentiation and function. However, keratinocyte production of $1,25(OH)_2D_3$ is thought to be mediated through the *CYP27B1* gene product (Fu *et al.*, 1997). Alternatively, a *CYP27B1*-independent pathway may catalyze local production of $1,25(OH)_2D_3$. However, *in vivo* and *in vitro* experiments argue against *CYP27B1*-independent synthesis of $1,25(OH)_2D_3$ in the skin. For example, VDR (L233S), a mutated form of VDR, which is incapable of binding $1,25(OH)_2D_3$, rescues the $VDR^{-/-}$ defect in hair-follicle cycling when expressed in basal keratinocytes of the $VDR^{-/-}$ mouse (Skorija *et al.*, 2005). The activity of VDR L233S supports the possibility that VDR activity in the skin is regulated by a previously unreported skin-selective ligand, or potentially no ligand at all. We recently showed *in vitro* evidence for a keratinocyte-selective, $1,25(OH)_2D_3$-independent transactivation by VDR that supports this idea (Ellison *et al.*, 2007). VDR activity is regulated by post-translational modifications such as phosphorylation. For example, okadaic acid, a protein phosphatase inhibitor, increases both $1,25(OH)_2D_3$-dependent and $1,25(OH)_2D_3$-independent activation of VDR by promoting interaction between VDR and the VDR-interacting protein 205 coactivators (Barletta *et al.*, 2002). Thus, it is possible that keratinocyte growth factor pathways may impinge on VDR to activate this nuclear receptor in keratinocytes through a $1,25(OH)_2D_3$-independent mechanism. Additional studies in this vein may produce novel strategies of targeting VDR pharmacologically in the skin.

Another key finding of these studies is that VDR protects against skin tumorigenesis induced by UV irradiation, the cause of skin cancer most relevant to human disease. $VDR^{-/-}$ mice exposed chronically to UV light developed tumors with a mean latency much shorter than that in wild-type controls (Figure 2a). The requirement for the $1,25(OH)_2D_3$ ligand in protecting against UV-induced tumorigenesis remains an open question. Since DMBA and UV radiation induce tumorigenesis by different mechanisms, it is possible that $1,25(OH)_2D_3$ may play a protective role here. Indeed, recent studies suggest that pharmacological application of vitamin D compounds may reduce cell death and enhance DNA repair in mouse skin following UV exposure (Dixon *et al.*, 2007). In that study, analogs selective for a non-genomic, VDR-independent signaling pathway were effective and this raised the intriguing possibility that the $1,25(OH)_2D_3$ ligand could protect against UV-induced skin tumorigenesis in a receptor-independent manner. This putative non-genomic pathway represents another paradigm in which actions of VDR and its $1,25(OH)_2D_3$ ligand may be uncoupled in skin physiology.

Early responses of keratinocytes to UV exposure and damage occur through p53-dependent and p53-independent pathways (Maltzman and Czyzyk, 1984; Lee *et al.*, 1997; Melino *et al.*, 2002). Data presented here indicate that VDR expression is not critical for UV-induced upregulation of p53 protein levels and activity in keratinocytes. Both total and phosphorylated p53 were upregulated to the same extent in $VDR^{-/-}$ and wild-type keratinocyte cultures (Figure 3). The intact p53-response pathway in $VDR^{-/-}$ keratinocytes predicts that DNA repair would be equal in wild-type and $VDR^{-/-}$ epidermis. However, thymine-dimer repair was

markedly attenuated in newborn $VDR^{-/-}$ epidermis as evidenced by the significantly higher levels of thymine dimers that remained in $VDR^{-/-}$ epidermis as compared with wild-type controls 24 hours following a single UV dose. Although it will be important to extend these studies to older animals, these studies clearly indicate that the $VDR^{-/-}$ mouse has defective DNA-repair pathways. Cumulatively, these data support a role for VDR in regulating one or more p53-independent mechanisms involved in UV-induced DNA damage repair.

UV causes a multi-step cascade of events in exposed cells (Matsumura and Ananthaswamy, 2002). Initially, cell growth is arrested so that DNA damage may be repaired. Those keratinocytes that harbor extensive cellular damage, which is beyond repair, undergo apoptosis. After an initial period of cell-cycle arrest, proliferation ensues in order to replace cells lost to apoptosis. As a result of hyperproliferation, the epidermis becomes thickened so that upper layers of the epidermis protect the basal layer of keratinocytes from future exposure to UV. Our data indicate that VDR may play important roles in each of these cellular responses to UV. For example, acute UV exposure reduced growth of wild-type keratinocytes, whereas $VDR^{-/-}$ keratinocytes remained more proliferative (Figure 5a and b). These data indicate that VDR is important for growth arrest immediately following UV exposure. Fewer apoptotic cells were detected *in vivo* in $VDR^{-/-}$ skin as compared with in $VDR^{+/+}$ skin following a single dose of UVB. This suggests that VDR also plays a role in detecting the need for apoptosis or is involved in executing the cell death process itself (Figure 6b). In either case, it is likely that damaged keratinocytes remain in $VDR^{-/-}$ skin following UV exposure. Following repeated UV exposures over a 2-week period, wild-type keratinocytes in the epidermis became more proliferative and epidermal thickness increased to a greater extent in wild-type skin as compared with in $VDR^{-/-}$ skin (Figure 7). These data suggest that $VDR^{-/-}$ mice are more sensitive to skin tumorigenesis induced by chronic UV treatment because they are unable to mount an effective thickening of their epidermal layer as compared with wild-type mice. Indeed, previous studies have illustrated an important role for epidermal thickening in protecting basal keratinocytes from subsequent DNA damage caused by UV (de Winter *et al.*, 2001). Finally, the enhanced basal proliferation of $VDR^{-/-}$ keratinocytes previously observed *in vivo* (Zinser *et al.*, 2002), and the reduced proliferation and epidermal thickening of $VDR^{-/-}$ keratinocytes in response to chronic UV, observed in these studies, indicate that VDR exerts opposing actions on these two distinct proliferative pathways. The identification of VDR-regulated genes involved in these pathways will be the next important goal. To this end, the $VDR^{-/-}$ keratinocyte cell system will prove extremely valuable.

MATERIALS AND METHODS

Animal maintenance

All studies were approved by the Institutional Animal Care and Use Committee at Case Western Reserve University. Mice lacking the *CYP27B1* gene ($CYP27B1^{-/-}$) (Dardenne *et al.*, 2001) and *VDR* gene ($VDR^{-/-}$) (Li *et al.*, 1997) were generously provided by R St-Arnaud (Shriners Hospital for Children, Montreal, Quebec) and M Demay (Massachusetts General Hospital and Harvard Medical School, Boston, MA), respectively. Both lines of mice are on a homogeneous C57BL/6 genetic background having been back-crossed greater than 10 times into this strain. $VDR^{-/-}$ $CYP27B1^{-/-}$ double knockout mice were generated by mating mice heterozygous for both the genes. Mouse genotyping was performed with tail DNA as previously described (Ellison *et al.*, 2007). Mice were fed a diet containing 2% calcium, 1.25% phosphorus, and 20% lactose supplemented with 2.2 IU of vitamin D_3 per gram (TD96348; Teklad, Madison, WI), which has been shown to normalize serum mineral homeostasis, skeletal growth, bone density, and body weight in $CYP27B1^{-/-}$ (Dardenne *et al.*, 2003) and $VDR^{-/-}$ mice (Li *et al.*, 1998).

Chemical carcinogen treatment and tumor monitoring

$VDR^{+/+}$, $VDR^{+/-}$, and $VDR^{-/-}$ mice ($n=7$ of each); $CYP27B1^{+/+}$, $CYP27B1^{+/-}$, and $CYP27B1^{-/-}$ mice ($n=11$ of each); and $VDR^{-/-}$ $CYP27B1^{-/-}$ double knockout mice ($n=12$) were treated with DMBA (100 mg kg^{-1} body weight) in corn oil by oral gavage at 5 and 6 weeks of age as described previously (Zinser *et al.*, 2002). Mice were examined weekly for tumor development by visual inspection and palpation. Mice bearing a skin growth 1 mm or larger, persisting for more than 7 days, were scored positive.

UVB irradiation and tumor monitoring

Dorsal skin was shaved with electric clippers and depilated with Nair lotion 24 hours before UVB exposure. Mice (5–7 weeks old at the onset of the study) were irradiated three times per week, with 2–3 days between treatments, and re-depilated as needed. The dorsal skin was exposed to UV irradiation from a band of six FS-40 fluorescent lamps; UVB and UVC wavelengths not normally present in natural solar radiation were filtered out from this UV light using Kodacel cellulose film. After filtration with a Kodacel film, the UVB wavelengths ranged from approximately 290 to 320 nm. UVB emission was monitored with an IL-443 phototherapy radiometer (International Light, Newburyport, MA) equipped with an IL SED 240 detector fitted with a W side angle quartz diffuser and a SC5 280 filter. The dose of UVB varied to maximize UV exposure with minimal ulceration of the skin. Mice received 120 mJ cm^{-2} for 2 weeks. The dose was then increased 25% per week for 5 weeks, reaching the maximal dose of 400 mJ cm^{-2}. This dose was administered for 9 weeks. With advancing age, the skin of several mice became increasingly ulcerated so the dose was reduced to 200 mJ cm^{-2} for the rest of the study. Mice received UVB treatments for 33 weeks, and were examined weekly for tumor development by visual inspection and palpation. Mice bearing a skin growth 1 mm or larger, persisting for more than 7 days, were scored positive.

Another cohort of mice (5–7 weeks old) were depilated as described above and exposed to 120 mJ cm^{-2}. Twenty-four hours later, mice were anesthetized with Avertin, and a biopsy was taken from the dorsal skin and fixed in neutral buffered formalin. Mice were exposed to five additional doses of UV and another sample of skin was collected. TUNEL staining was performed on the skin samples following the first dose of UV, and PCNA staining and epidermal thickness measurement was performed on all skin samples, as described below.

Tumor classification

Tumors were collected at death or by excision biopsy, fixed in neutral buffered formalin, and embedded in paraffin. Sections measuring 5 μm were stained with hematoxylin and eosin, and evaluated in a blinded manner. DMBA tumors were classified as a sebaceous hyperplasia if more than 90% of the cells were well-differentiated mature sebocytes, or sebaceous adenoma if approximately 50% of the cells were well-differentiated mature sebocytes. UV-induced tumors were classified as a papilloma, either benign or with mild, moderate, or severe dysplasia, as a SCC, either *in situ* or invasive, or as an AFX. Benign papillomas had few to no mitotic structures above the basal epidermal layer and no cytological atypia. Mild, moderate, and severe atypia papillomas had parakeratin, increasing numbers of mitotic figures above the basal layer, and increasing likelihood of cytological atypia. SCC *in situ* was characterized by parakeratosis, and high likelihood of hyperkeratosis, dyskeratosis, and acanthosis. There were many atypical keratinocytes with hyperchromatism, pleomorphism, atypical mitoses, and loss of orderly maturation (sometimes creating a ''windblown'' appearance). In some cases, the epidermis showed evidence of a loss of polarity. Invasive SCC was characterized by the descriptors mentioned above for SCC *in situ*, with the addition of invasion of the dermis by atypical keratinocytes and the lack of a defined basal layer. Some mice developed rapidly growing tumors consisting of dermal proliferation of atypical spindle cells, epithelioid cells, or multinucleated giant cells, and, sometimes, foamy cells often extending up against the epidermis. Tumors contained severe pleomorphism, hyperchromatism, and many very atypical mitoses, consistent with AFX.

Immunoblotting

Primary mouse keratinocytes were isolated as previously described (Ellison *et al.*, 2007) and cultured in keratinocyte-serum-free medium (Invitrogen, Carlsbad, CA) on collagen-I plates (Corning, Lowell, MA). Cells were exposed to UVB through a thin film of phosphate-buffered saline (PBS) and media were replaced. Protein was harvested in sample buffer (62.5 mM Tris (pH 6.8), 10% glycerol, 2% sodium dodecyl sulfate) and protein concentration was determined by BCA assay (Pierce, Rockford, IL). β-Mercaptoethanol (1%) and bromphenol blue (0.01%) were added and equal amounts of protein were separated on polyacrylamide gels. Protein was transferred to polyvinylidene difluoride membrane (Immobilon-P; Millipore, Billerica, MA) and probed for p53 (sc-6243, 1:400; Santa Cruz Biotechnology, Santa Cruz, CA), phospho-serine15 p53 (1:1,000; Cell Signaling Technology, Danvers, MA), or actin (1:20,000; Sigma-Aldrich, St Louis, MO). Membranes were washed and probed with the species appropriate secondary antibody at a 1:10,000 dilution, and then the signal was visualized by chemiluminescence.

Slot-blot analysis of thymine dimers

Newborn $VDR^{+/+}$ and $VDR^{-/-}$ mice were treated with 120 mJ cm^{-2} of UV and skin was harvested at the indicated time points. Unirradiated skin was also collected as a control. Skin was floated in dispase (BD Biosciences, Bedford, MA) for 20 minutes at 37 C, and then the epidermis was removed with forceps. Epidermis was digested overnight in lysis solution with proteinase K (supplied with the kit) and genomic DNA was purified using DNeasy columns (Qiagen Inc., Valencia, CA). Prior to DNA purification, the solution was treated for 2 minutes at room temperature with RNaseA (2 μg μl^{-1}; Sigma-Aldrich). After elution, DNA was further purified by standard phenol/chloroform extraction and ethanol precipitation. DNA concentration was determined using a spectrophotometer.

DNA was denatured by boiling in 0.4 M NaOH/10 mM EDTA for 10 minutes. Ice-cold ammonium acetate (2 M) was added to a final concentration of 1 M. A 50 ng weight per well of DNA was spotted onto a wet nitrocellulose membrane (Biotrace NT; VWR International, West Chester, PA) using a Bio-Dot SF apparatus (Bio-Rad Laboratories, Hercules, CA). The membrane was washed with 0.4 M NaOH/10 mM EDTA, removed from the apparatus, and baked under vacuum for 30 minutes at 80 °C. The membrane was incubated with a primary antibody recognizing thymine dimers (1:2500, clone KTM53; Kamiya Biomedical Company, Seattle, WA), followed by washing and incubation with a goat anti-mouse secondary antibody (1:10,000; KPL, Gaitherburg, MD). Signal was visualized by chemiluminescence. Thymine-dimer signal was normalized to total genomic DNA by probing with radiolabeled mouse genomic DNA. Genomic DNA was ^{32}P labeled using the Prime-a-Gene kit (Promega, Madison, WI) according to the manufacturer's instructions.

MTT assay

Primary mouse keratinocytes were isolated and cultured as described above. Twenty-four hours after plating, cells were exposed to UV through a thin film of PBS and media were replaced. Proliferation rate was measured at the indicated time periods by incubating cells with MTT (3-(4,5-dimethylthiazol-2-yl)-2,5-diphenyltetrazolium bromide, 0.5 mg ml^{-1} final concentration) for 1 hour. Cells were washed twice with PBS and cells were lysed with isopropanol with 0.04 N HCl. Absorbance at 560 nm was measured using a plate spectrophotometer.

Histological analysis of skin

Epidermal thickness was calculated from 20–25 measurements from multiple fields of paraffin-embedded skin sections immunohistochemically stained for PCNA expression, and viewed at an original magnification of ×100. Measurements were made using Axiovision software (Carl Zeiss, Thornwood, NY). Differences in thickness were analyzed by the two-tailed Student's *t*-test in Microsoft Excel.

Immunohistochemistry was performed with paraffin-embedded sections using Vectastain avidin–biotin peroxidase and peroxidase DAB kits (Vector Laboratories, Burlingame, CA). Briefly, skin sections were deparaffinized with xylene and rehydrated in ethanol at decreasing concentrations. Sections were boiled for 20 minutes in 10 mM citrate buffer, pH 6, for antigen retrieval, and endogenous peroxidase was blocked using 3% H_2O_2. For PCNA staining, sections were blocked in PBS with 1.5% horse serum, followed by overnight incubation with the primary antibody (PCNA sc-56; Santa Cruz Biotechnology), followed by a biotinylated horse anti-mouse secondary antibody (1:200; Vector Laboratories) and conjugation with the avidin–biotin peroxidase complex. Sections were counterstained with Gill's hematoxylin #2 (Fisher Scientific, Pittsburgh, PA), dehydrated, cleared, and mounted in Permount. A control (buffer without primary antibody) was performed for each tissue stained.

Apoptotic cells were detected in paraffin-embedded skin sections using the DeadEnd Fluorometric TUNEL system (Promega) according to the manufacturer's instructions, with the following exceptions: tissue sections were not fixed again following rehydration and tissue was not treated with proteinase K. Instead, tissue was microwaved

for 1 minute at high power in 100 mM citrate buffer, pH 6, and then incubated for 30 minutes in Tris-HCl, pH 7.5, containing 3% BSA and 20% normal bovine serum. Slides were washed twice in PBS before continuing with the manufacturer's labeling protocol. Coverslips were mounted on slides with Vectashield mounting medium containing 4,6-diamino-2-phenylindole (Vector Laboratories).

CONFLICT OF INTEREST

The authors state no conflict of interest.

ACKNOWLEDGMENTS

We thank Tom McCormick and members of the laboratories of Drs Ruth Keri and Richard Eckert for providing guidance for the design and execution of the experiments presented here. This work was supported by National Institutes of Health Grant R01DK53980 and by a Pilot and Feasibility seed grant from the Skin Disease Research Center at Case Western Reserve University (AR639750, to PNM). TIE was supported by NIGMS, National Institutes of Health, Institutional National Research Service Award T32GM 08803.

REFERENCES

Albert MR, Weinstock MA (2003) Keratinocyte carcinoma. *CA Cancer J Clin* 53:292–302

Barletta F, Freedman LP, Christakos S (2002) Enhancement of VDR-mediated transcription by phosphorylation: correlation with increased interaction between the VDR and DRIP205, a subunit of the VDR-interacting protein coactivator complex. *Mol Endocrinol* 16:301–14

Bikle DD (2004) Vitamin D and skin cancer. *J Nutr* 134:3472S–8S

Bikle DD, Chang S, Crumrine D, Elalieh H, Man MQ, Choi EH *et al.* (2004) 25 Hydroxyvitamin D 1 alpha-hydroxylase is required for optimal epidermal differentiation and permeability barrier homeostasis. *J Invest Dermatol* 122:984–92

Bikle DD, Nemanic MK, Whitney JO, Elias PW (1986) Neonatal human foreskin keratinocytes produce 1,25-dihydroxyvitamin D3. *Biochemistry* 25:1545–8

Cheskis B, Freedman LP (1994) Ligand modulates the conversion of DNA-bound vitamin D_3 receptor (VDR) homodimers into VDR-retinoid X receptor heterodimers. *Mol Cell Biol* 14:3329–38

Chida K, Hashiba H, Fukushima M, Suda T, Kuroki T (1985) Inhibition of tumor promotion in mouse skin by 1 alpha,25-dihydroxyvitamin D_3. *Cancer Res* 45:5426–30

Dardenne O, Prud'homme J, Arabian A, Glorieux FH, St-Arnaud R (2001) Targeted inactivation of the 25-hydroxyvitamin D(3)-1(alpha)-hydroxylase gene (CYP27B1) creates an animal model of pseudovitamin D-deficiency rickets. *Endocrinology* 142:3135–41

Dardenne O, Prud'homme J, Hacking SA, Glorieux FH, St-Arnaud R (2003) Correction of the abnormal mineral ion homeostasis with a high-calcium, high-phosphorus, high-lactose diet rescues the PDDR phenotype of mice deficient for the 25-hydroxyvitamin D-1alpha-hydroxylase (CYP27B1). *Bone* 32:332–40

de Winter S, Vink AA, Roza L, Pavel S (2001) Solar-simulated skin adaptation and its effect on subsequent UV-induced epidermal DNA damage. *J Invest Dermatol* 117:678–82

Dixon KM, Deo SS, Norman AW, Bishop JE, Halliday GM, Reeve VE *et al.* (2007) *In vivo* relevance for photoprotection by the vitamin D rapid response pathway. *J Steroid Biochem Mol Biol* 103:451–6

Ellison TI, Eckert RL, MacDonald PN (2007) Evidence for 1,25-dihydroxyvitamin D3-independent transactivation by the vitamin D receptor: uncoupling the receptor and ligand in keratinocytes. *J Biol Chem* 282: 10953–62

Erben RG, Soegiarto DW, Weber K, Zeitz U, Lieberherr M, Gniadecki R *et al.* (2002) Deletion of deoxyribonucleic acid binding domain of the vitamin D receptor abrogates genomic and nongenomic functions of vitamin D. *Mol Endocrinol* 16:1524–37

Fu GK, Lin D, Zhang MY, Bikle DD, Shackleton CH, Miller WL *et al.* (1997) Cloning of human 25-hydroxyvitamin D-1 alpha-hydroxylase and mutations causing vitamin D-dependent rickets type 1. *Mol Endocrinol* 11:1961–70

Gray RW, Omdahl JL, Ghazarian JG, DeLuca HF (1972) 25-Hydroxycholecalciferol-1-hydroxylase. Subcellular location and properties. *J Biol Chem* 247:7528–32

Holick MF (2007) Vitamin D deficiency. *N Engl J Med* 357:266–81

Hughes MR, Malloy PJ, Kieback DG, Kesterson RA, Pike JW, Feldman D *et al.* (1988) Point mutations in the human vitamin D receptor gene associated with hypocalcemic rickets. *Science* 242:1702–5

Johns HE, Pearson ML, Leblanc JC, Helleiner CW (1964) The ultraviolet photochemistry of thymidylyl-(3′–5′)-thymidine. *J Mol Biol* 9:503–24

Kerner SA, Scott RA, Pike JW (1989) Sequence elements in the human osteocalcin gene confer basal activation and inducible response to hormonal vitamin D3. *Proc Natl Acad Sci USA* 86:4455–9

Kliewer SA, Umesono K, Mangelsdorf DJ, Evans RM (1992) Retinoid X receptor interacts with nuclear receptors in retinoic acid, thyroid hormone and vitamin D3 signalling. *Nature* 355:446–9

Lee H, Larner JM, Hamlin JL (1997) A p53-independent damage-sensing mechanism that functions as a checkpoint at the G1/S transition in Chinese hamster ovary cells. *Proc Natl Acad Sci USA* 94:526–31

Li YC, Amling M, Pirro AE, Priemel M, Meuse J, Baron R *et al.* (1998) Normalization of mineral ion homeostasis by dietary means prevents hyperparathyroidism, rickets, and osteomalacia, but not alopecia in vitamin D receptor-ablated mice. *Endocrinology* 139:4391–6

Li YC, Pirro AE, Amling M, Delling G, Baron R, Bronson R *et al.* (1997) Targeted ablation of the vitamin D receptor: an animal model of vitamin D-dependent rickets type II with alopecia. *Proc Natl Acad Sci USA* 94:9831–5

Maltzman W, Czyzyk L (1984) UV irradiation stimulates levels of p53 cellular tumor antigen in nontransformed mouse cells. *Mol Cell Biol* 4:1689–94

Matsumura Y, Ananthaswamy HN (2002) Short-term and long-term cellular and molecular events following UV irradiation of skin: implications for molecular medicine. *Expert Rev Mol Med* 2002:1–22

Melino G, De Laurenzi V, Vousden KH (2002) p73: friend or foe in tumorigenesis. *Nat Rev Cancer* 2:605–15

Panda DK, Miao D, Tremblay ML, Sirois J, Farookhi R, Hendy GN *et al.* (2001) Targeted ablation of the 25-hydroxyvitamin D 1alpha-hydroxylase enzyme: evidence for skeletal, reproductive, and immune dysfunction. *Proc Natl Acad Sci USA* 98:7498–503

Petrocelli T, Poon R, Drucker DJ, Slingerland JM, Rosen CF (1996) UVB radiation induces p21Cip1/WAF1 and mediates G1 and S phase checkpoints. *Oncogene* 12:1387–96

Sakai Y, Demay MB (2000) Evaluation of keratinocyte proliferation and differentiation in vitamin D receptor knockout mice. *Endocrinology* 141:2043–9

Setlow RB, Setlow JK (1962) Evidence that ultraviolet-induced thymine dimers in DNA cause biological damage. *Proc Natl Acad Sci USA* 48:1250–7

Siliciano JD, Canman CE, Taya Y, Sakaguchi K, Appella E, Kastan MB (1997) DNA damage induces phosphorylation of the amino terminus of p53. *Genes Dev* 11:3471–81

Skorija K, Cox M, Sisk JM, Dowd DR, MacDonald PN, Thompson CC *et al.* (2005) Ligand-independent actions of the vitamin D receptor maintain hair follicle homeostasis. *Mol Endocrinol* 19:855–62

St-Arnaud R, Messerlian S, Moir JM, Omdahl JL, Glorieux FH (1997) The 25-hydroxyvitamin D 1-alpha-hydroxylase gene maps to the pseudovitamin D-deficiency rickets (PDDR) disease locus. *J Bone Miner Res* 12:1552–9

Van Cromphaut SJ, Dewerchin M, Hoenderop JG, Stockmans I, Van Herck E, Kato S *et al.* (2001) Duodenal calcium absorption in vitamin D receptor-knockout mice: functional and molecular aspects. *Proc Natl Acad Sci USA* 98:13324–9

Yoshizawa T, Handa Y, Uematsu Y, Takeda S, Sekine K, Yoshihara Y *et al.* (1997) Mice lacking the vitamin D receptor exhibit impaired bone formation, uterine hypoplasia and growth retardation after weaning. *Nat Genet* 16:391–6

Zinser GM, Sundberg JP, Welsh J (2002) Vitamin D_3 receptor ablation sensitizes skin to chemically induced tumorigenesis. *Carcinogenesis* 23:2103–9